that HCN would relax CO with a probability of about 5×10^{-4}, which in a mixture, HCN/CO = 1/7, at 90 mtorr, would give a relaxation time of 35 ms. This is a very long time to "store" the 2100 cm^{-1} per molecule, which is available to be fed back into the HCN (100) state. For the 6% of the molecules which are in (010) [at 300 K] this feeds the upper state of the $(11^10) \rightarrow (04^00)$ laser oscillation.

This calculated 35-ms inversion lifetime is consistent with the observations of the oscillations. When the relations (3) are used with the observed $T_0 = 400$ μs, $T_d = 850$ μs with $\tau = 35$ ms, the photon cavity lifetime t_c comes out to be 9.5×10^{-6} s and the incremental gain constant $g = 0.029$ m^{-1}. Thus, although the origin of these oscillations with CO dilution has not been proved to be due to the energy storage suggested, this does seem to fit the observations quite well. It is also clear why there was no isotopic effect when $C^{18}O$ was substituted for $C^{16}O$. Although the energy match was better, and the transfer rate undoubtedly improved, the effect would have been to alter the inversion lifetime, τ, upon which the observed times T_d and T_0 only very weakly depend. Eliminating a between eq 3 we have

$$\frac{4\pi^2\tau t_c}{T_0^2} = \frac{2\tau}{T_d} - 1$$

and since $2\tau/T_d$ is large compared to one, τ can be cancelled to within 2% error and $T_0^2/T_d \approx 2\pi^2 t_c$. Given the electric dipole moment of 3.0 D for HCN, one can estimate the spontaneous emission lifetime for a transition of this frequency[12] to be 9 s. Taking this with the above-calculated cavity lifetime of $t_c = 9.5 \times 10^{-6}$ s and a line width of 2 MHz, one calculates[13] $\Delta N \approx 10^6$ cm^{-3} for the threshold inversion. The photon lifetime calculated from the relaxation oscillations is an apparent one, sustained by the energy storage of CO. It is not a property of the cavity. If one were to take the position that the threshold inversion and the incremental gain obtained from the relaxation oscillations could reasonably be considered steady-state properties of the HCN lasing system in the absence as well as the presence of the CO, then a natural photon cavity lifetime could be estimated from $t_c = 1/cg$ to be 10^{17} s.

Conclusion

The output characteristics of a flashlamp-pumped HCN gas laser have been interpreted on the basis of initial excitation of ν_3, the CH stretch, by the infrared tail of the flashlamps, followed by collisional transfer to $(\nu_1 + \nu_2)$, the upper laser level. This picture led to a calculation of the time evolution of the inversion which largely mimics the time behavior of the submillimeter output pulse. Interpretation of some long-time output modulation of the pulse tail by added CO yielded cavity parameters which agreed well with the inversion evolution based solely upon known and closely estimated energy transfer rates. Although proof of this picture cannot be offered, internal consistency of loosely related phenomena provides good reason for confidence in the results.

Acknowledgment. The author thanks the Department of Energy, Office of Basic Energy Sciences, for support of this research, Harris J. Silverstone for a valuable discussion, and especially Nabil M. Lawandy for his long time interest in and expert input into this work.

Registry No. HCN, 74-90-8; CO, 630-08-0.

(11) J. T. Yardley, "Introduction to Molecular Energy Transfer", Academic Press, New York, 1980, p 89.
(12) W. H. Flygare, "Molecular Structure and Dynamics", Prentice-Hall, Englewood Cliffs, New Jersey, 1978, p 113.
(13) A. Yariv, "Quantum Electronics", Wiley, New York, 1975, p 179.

Analysis of Protein–Lipid Interactions Based on Model Simulations of Electron Spin Resonance Spectra

Eva Meirovitch,[†‡] Akbar Nayeem,[†] and Jack H. Freed*[†]

Baker Laboratory of Chemistry, Cornell University, Ithaca, New York 14853, and Isotope Department, The Weizmann Institute of Science, 76100 Rehovot, Israel *(Received: February 9, 1984)*

ESR spectra from protein-containing lipid dispersions have been interpreted in the past primarily in terms of two nitroxide species related respectively to "fluid" and "immobile" phospholipid environments. In this report we consider interpretations based primarily on a single type of lipid, for the two cases of spin-probe-doped membranes and of chemically labeled membrane proteins. The doped membranes are viewed as bilayer fragments with considerable local order but with macroscopic disorder of such fragments in the dispersion. In this "one-site" model all lipids are similar. They are fluid and oriented in their local environment. This model does *not* require a second species immobilized by contact with the proteins. The labeled proteins are considered as very slowly reorienting macromolecular complexes such that the dynamic effects on the ESR spectrum arise mainly from faster internal processes. The importance of, and the potential inherent in, detailed spectral simulation based on well-conceived models are emphasized by illustrating the great range of spectral line shapes that these models can yield with suitable parameters. Simulations are compared with some recent experimental examples previously interpreted in terms of a two-site model. Reasonably good results are obtained for spin-probe-doped membranes when allowance is made for local ordering as well as for some distortion of the alkyl chain ends. Such effects are modeled by introducing an ordering potential λ and a diffusion tilt angle Ψ which describes the tilt of the nitroxide moiety relative to the rest of the alkyl chain. The effects of adding protein or of lowering the temperature are modeled by increasing the local ordering while decreasing somewhat the motional rates with some increase in alkyl chain distortions. In the case of spin-labeled membrane proteins, the model of very anisotropic rotation, in which the side chain containing the nitroxide is rotating more rapidly than the protein about an effective axis tilted relative to the N–O axis, is found to account for the extra splittings with just a single-site model.

I. Introduction

The model of a boundary layer of lipids coating a protein molecule is based, to a large extent, on the interpretation of the ESR spectra from spin probes (mainly nitroxide free radicals) doped into biological or reconstituted membranes or from systems wherein membrane proteins have been labeled chemically with a paramagnetic moiety. In many cases, one observes what appears to be two (or more) superimposed ESR spectra corresponding to a population of "fluid" lipids and to one (or more) species of

[†] Cornell University.
[‡] Weizmann Institute of Science.

0022-3654/84/2088-3454$01.50/0

"immobilized" boundary lipids.[1-15]

On the other hand, evidence from other techniques such as NMR and fluorescent probe studies, as well as from a few ESR measurements, is not necessarily consistent with the concept of a distinct boundary lipid layer. This matter has been cogently reviewed by Chapman et al.,[2] who points out that the NMR studies (using ^1H, ^{19}F, or ^2H nuclei) do not show the occurrence of two types of lipids but are instead consistent with "continuity between the bulk lipid phase and the boundary layer lipids [with] ready diffusion between these lipids [taking] place." Seelig and Seelig, in their review of the ^2H NMR reconstitution studies,[16] also note that they are all consistent with "only one homogeneous lipid environment [being] present above T_c even when a substantial amount of protein is present." NMR is generally regarded as a method which samples longer time scales compared to ESR and other methods such as fluorescence. Jähnig[17] has analyzed the results of fluorescence experiments on the lipid–protein interaction and concludes that "proteins induce a higher orientational order of the surrounding lipid molecules" in what he calls "off-normal directions", i.e., increased ordering at an angle that is tilted relative to the bilayer normal. Increased ordering of lipid chains has also been suggested by Chapman et al.[2] for lower protein concentrations, but they suggest a disordering effect at higher concentrations. However, Jähnig's interpretation is that the ordering is in the off-normal directions, due to the local-order parameters, which however are fluctuating in time (and there is also lateral diffusion to sites of different instantaneous local order), so the NMR senses the longer time average, wherein the instantaneous local order has been averaged out. More recently, Paddy et al.[18] have examined their NMR results in terms of the possibility of a long-time average over lipid exchange between two types of sites but point out that this is only one of several interpretations. Such time averaging is also suggested by Seelig and Seelig,[16] but they note puzzling aspects regarding the ESR of spin-labels covalently attached to a membrane protein (see also ref 2). Devaux[15] has recently reviewed the case for interpretation of NMR results in terms of the two-species model.

To summarize this brief review, it has apparently not been possible so far to set up an unambiguous picture, consistent with all the physical measurements. As far as ESR is concerned, there are cases wherein the arguments supporting one or the other of the two extreme interpretations outlined above are cogent; in other cases, however, the reasoning underlying the interpretation of the spectra is uncertain.

The premise of the multisite model lies mainly in dominant features of the ESR line shape, which become regarded as "typical". The "fluid" population has been consistently associated with the common nitroxide triplet observed for molecules reorienting in a nearly isotropic medium (i.e., one that does not impose local ordering on the spin probes). Absorption peaks at low and high fields were unequivocally assigned to a second spectral component of "immobilized" nitroxides. When the separation between the outer peaks equals roughly $2A_{zz'}$ (with $A_{zz'}$ denoting the maximum hyperfine splitting), an interpretation in terms of nitroxides which are practically static on the ESR time scale, giving rise to an isotropic rigid-limit powder pattern, was offered. For a reduced peak separation, the radicals associated with this second component were regarded as "partially immobilized"; in some cases, changes in the slope of the derivative ESR curve were interpreted as additional spectral components associated with species immobilized to various extents (for example, see ref 2 and 14).

Arguments favoring the two-site model are (a) the invariance of the positions in the field, but not of the relative intensity, of the outer "immobile" and the inner "fluid" $m = \pm 1$ components flanking the central $m = 0$ line upon varying sample temperature or composition (i.e., the lipid to protein ratio) and (b) the ability to separate experimentally the two spectral components by preparing samples wherein the spin probes are either all "fluid" or all "immobile" (see, for example, ref 10).

The similarity of the ESR spectra obtained from lipid dispersions in the absence and in the presence of the membrane proteins[19] is strongly supportive of a homogeneous population of lipids. Even when previous interpretations invoked a single nitroxide species, only in a very few cases have quantitative spectral analyses been offered.[20]

In previous work[21] we found that dispersions of pure lipids could lead to ESR spectra strikingly similar to ones obtained from labeled biological membranes that had been interpreted in terms of the two-site model. Our analysis of the spectra from pure lipids suggested an alternative interpretation in terms of a single-species model.

In the present work we consider in some detail two single-species models, which are related, for interpreting ESR spectra from membranes in terms of appropriate dynamic, ordering, and conformational characteristics.

The first model is a general and comprehensive approach that considers lyotropic liquid crystalline lipid structures as collections of bilayer fragments dispersed isotropically in space. Within a given fragment, the liquid crystalline director is oriented uniformly; i.e., substantial "microscopic order" prevails, whereas the morphology is typically one of "macroscopic disorder". We denote this model as MOMD (microscopic order–macroscopic disorder). In this formulation rotational rates, ordering parameters, and the relative orientation of diffusion (ordering) and magnetic axes are the independent molecular variables required to simulate ESR spectra.[22,23] This model is basically the one suggested previously.[21,24] We have, in the present work, carried out a detailed study of spectral sensitivity with respect to the various physical constants and examined the applicability of the MOMD model.

The second approach is applicable for *labeled* macromolecules, where the nitroxide moiety is bound selectively to the protein. The relevant theory was formulated some years ago by Mason et al.[25] and has been applied successfully to interpret ESR spectra from end-labeled (with a piperidine radical) poly(benzyl glutamate) polymers.[25] It is assumed that the overall Brownian motion of the macromolecule is relatively slow on the ESR time scale but

(1) Cable, M. B.; Powell, G. L. *Biochemistry* **1980**, *19*, 5679.
(2) Chapman, D.; Gomez-Fernandez, J. C.; Goni, F. M. *FEBS Lett.* **1979**, *98*, 211.
(3) Davoust, J.; Schoot, B. M.; Devaux, Ph. F. *Proc. Natl. Acad. Sci. U.S.A.* **1979**, *76*, 2755.
(4) Davoust, J.; Bienvenue, A.; Fellman, P.; Devaux, Ph. F. *Biochim. Biophys. Acta* **1980**, *596*, 28.
(5) Fretten, P.; Morris, S. J.; Watts, A.; Marsh, D. *Biochim. Biophys. Acta* **1980**, *598*, 247.
(6) Jost, P. C.; Griffith, O. H. *Methods Enzymol.* **1978**, *49*, 369.
(7) Jost, P. C.; Griffith, O. H.; Capaldi, R. A.; Vanderkooi, G. *Proc. Natl. Acad. Sci. U.S.A.* **1973**, *70*, 480.
(8) Jost, P. C.; Griffith, O. H.; Capaldi, R. A.; Vanderkooi, G. *Biochim. Biophys. Acta* **1973**, *311*, 141.
(9) Jost, P. C.; Nadakauukaren, K. K.; Griffith, O. H. *Biochemistry* **1977**, *16*, 311.
(10) Knowles, P. F.; Watts, A.; Marsh, D. *Biochemistry* **1979**, *18*, 4480.
(11) Landgraf, W. C.; Inesi, G. *Arch. Biochem. Biophys.* **1969**, *130*, 111.
(12) Coan, C. R.; Keating, S. *Biochemistry* **1982**, *21*, 3214.
(13) Champeil, P.; Büschlen-Boucly, S.; Bastide, F.; Gary-Bobo, C. *J. Biol. Chem.* **1978**, *253*, 1179.
(14) Coan, C. R.; Inesi, G. *J. Biol. Chem.* **1977**, *252*, 3044.
(15) Devaux, P. F. "Biological Magnetic Resonance", Berliner, L. J., Reuben, J., Eds.; Plenum Press: New York, 1983.
(16) Seelig, J.; Seelig, A. *Q. Rev. Biophys.* **1980**, *13*, 19.
(17) Jähnig, F. *Proc. Natl. Acad. Sci. U.S.A.* **1979**, *76*, 6361.
(18) Paddy, M. R.; Dahlquist, F. W.; Davis, J. H.; Bloom, M. *Biochemistry* **1981**, *20*, 3152.
(19) Hauser, H.; Ganis, N.; Seneza, G.; Spiess, M. *Biochemistry* **1982**, *21*, 5621.
(20) Cannon, B.; Polnaszek, C. F.; Butler, K. W.; Göran-Eriksson, L. E.; Smith, I. C. P. *Arch. Biochem. Biophys.* **1975**, *167*, 505.
(21) Meirovitch, E.; Freed, J. H. *J. Phys. Chem.* **1980**, *84*, 3281.
(22) (a) Moro, G.; Freed, J. H. *J. Phys. Chem.* **1981**, *84*, 2837; (b) Moro, G.; Freed, J. H. *J. Chem. Phys.* **1981**, *74*, 3757.
(23) (a) Meirovitch, E.; Freed, J. H. *J. Phys. Chem.* **1980**, *84*, 2459; (b) Meirovitch, E.; Igner, E.; Moro, G.; Freed, J. H. *J. Chem. Phys.* **1982**, 77, 3915; (c) Meirovitch, E.; Freed, J. H. *J. Phys. Chem.*, in press.
(24) In liquid crystalline media, the fact that macroscopic disorder requires a superposition of spectra for all orientations was also considered by Seelig (cf. ref 28, Chapter 10).
(25) Mason, R. P.; Polnaszek, C. F.; Freed, J. H. *J. Phys. Chem.* **1974**, *78*, 1324.

there is more rapid internal rotation. The orientation of the axis of internal rotation, as well as the dynamic parameters, are to be determined in the analysis. We shall denote this model as VAR—very anisotropic reorientation (see ref 25 and 26). We point out below that in the limit of very high ordering the MOMD model becomes nearly identical with the VAR model in its spectral predictions.

We have selected from the published literature ESR spectra from a biological membrane doped with NO-labeled stearic acids and from a selectively labeled membrane protein and analyzed these with the MOMD and VAR models, respectively. In both cases, the two-site approach was adopted previously to interpret the ESR spectra.

With both models we treat ordering, fluidity, and molecular conformation in a physically reasonable and comprehensive manner. Our models, while consistent with results of the other techniques, are contrary to the multispecies model. Also they are in the spirit of Seelig and Seelig,[16] who have stated that "the correlation between chain *order* and chain *mobility* is not well understood as yet and it is thus important to keep the two concepts apart."

We also wish to note that only with the advent of our newer computational algorithms[22,23] has it become convenient to perform the extensive simulations (based upon rigorous slow-motional line shape theory) required for these apparently simple models. Perhaps the single most significant point that we wish to make in this study is the importance of detailed spectral simulations based upon well-defined microscopic models in the interpretation of ESR results, and the existence of powerful methods to carry this out.

In section II we discuss the method for calculating the spectra. In section III we present illustrative calculated spectra and we offer a reinterpretation of several experimental spectra. Further discussion and a summary are given in section IV.

II. Background

Before presenting our simulations, we wish to briefly summarize the features of ESR spectra in the presence of local ordering and macroscopic disorder. Local ordering means that the radical reorients in the presence of an orienting potential set up by the surrounding liquid crystalline medium and characterized by a director $\vec{d}$. Since there is no macroscopic order in a dispersion, $\vec{d}$ will be distributed at random relative to the external magnetic field $\vec{B}$. To calculate the overall ESR spectrum, one therefore has to calculate spectra for various tilt angles between $\vec{B}$ and $\vec{d}$[22] (see also ref 21 and 24) and convolute them according to the random distribution.

In these simulations we distinguish four principal coordinate systems: (1) the laboratory axes determined by $\vec{B}$: x, y, z; (2) the local coordinate system determined by $\vec{d}$: x'', y'', z''; (3) the molecular axes determined by the principal axes for ordering of the molecules relative to $\vec{d}$ as well as by the principal axes for molecular diffusion: x', y', z' (these axes are usually taken as coincident and determined to a considerable extent by symmetry); (4) the molecular axes determined by the principal axes of the magnetic tensors **A** and **g**: x''', y''', z'''. In general, none of these four sets of axes is coincident.

The model of microscopic order but macroscopic disorder first involves specifying the microscopic ordering of the lipids relative to $\vec{d}$ in terms of order parameter(s) and also the fluidity in terms of a rotational diffusion tensor, which can incorporate internal motions is necessary. Then one calculates the ESR spectrum for each value of $\theta = \cos^{-1}(\vec{B}\cdot\vec{d}/|B|)$, where $0° \leq \theta \leq 180°$ (or by symmetry one need only let $0° \leq \theta \leq 90$), and averages them over the unit sphere.

The relative orientation of the main diffusion axis z' in the magnetic frame $x'''y'''z'''$ is adjustable. As $x'y'z'$ is an axial coordinate frame, a polar angle Ψ and an azimuthal angle ϕ completely specify the spatial orientation of z'. We shall be mainly concerned in the following with varying Ψ and will often refer to this angle as "diffusion tilt".

TABLE I: Magnetic Parameters

	$A_{x'''}$, G	$A_{y'''}$, G	$A_{z'''}$, G	$g_{x'''}$	$g_{y'''}$	$g_{z'''}$
A[a]	6.34	5.83	33.9	2.0088	2.0061	2.0027
B[b]	5.89	5.42	31.42	2.0088	2.0061	2.0027

[a] From ref 28, p 570. [b] From ref 21.

The VAR model has been described in detail by Mason et al.[25] and Campbell et al.[26] For the convenience of the reader, we only review its basic physical assumptions.

Here one assumes that the whole macromolecule reorients slowly with a usually axial rotational diffusion tensor, specified by the motional rates $R_\perp$ and $R_\parallel$. The nitroxide side chain rotates at a more rapid rate with internal rotational diffusion coefficient R_I about a mean diffusion axis z'. The nature of the motions and the spectral sensitivity are such that simpler limiting cases usually apply.[26] In particular, it is often sufficient to take $R_\perp$ as a measure of the overall reorientation of the macromolecule, while $R_I \gg R_\perp$. (In such cases R_I has a nearly equivalent effect on the spectrum as $R_\parallel$, so we can formally regard R_I as an "effective" $R_\parallel$.) In the spectral analysis, one can then determine $R_\perp$, R_I and the angles Ψ and ϕ.

III. Results and Discussion

Magnetic Parameters. Throughout this study we have used two sets of magnetic parameters with the following arguments underlying their choice.

Series A is a typical set of parameters obtained from lyophilized nitroxide-labeled bovine serum albumin.[28] These are rather high values, corresponding to an isotropic hyperfine constant of 15.2 G. The second set B corresponds to a lower isotropic value of 14.2 G, the ratio of the corresponding individual hyperfine constants of sets A and B being 1.08. The set B parameters were used previously for NO-labeled dipalmitoylphosphatidylcholine (DPPC) dissolved in low water content DPPC bilayers,[21] which gave ESR spectra very similar to those obtained from the spin-probe-doped purple membrane of *Halobacterium halobium*[29] to be discussed below. In particular, we carried out extensive simulations for the 1,14 stearic acid probe, which is known to be associated with relatively low values of the hyperfine parameters, in agreement with a near to the methyl end labeled molecule.[30] Values as low as 14 G for the isotropic splitting of 1,14 stearic acid dissolved in membranes were assigned in former studies, which, following the usual "scaling" procedure, would correspond to $A_{z'''} = 29.9$ G. However, we find that in the purple membrane, $A_{z'''}$ must be higher (we estimate from Chignell and Chignell's paper[29] the extreme splitting in the still dynamic 50 °C spectrum to be 30.5 G and by extrapolation to the rigid-limit pattern, we obtain $A_{z'''} = 31.4$ G, in accord with set B).

The two sets of magnetic parameters A and B roughly span the range of hyperfine constants encountered with NO-labeled alkyl chains dissolved in model and biological membranes.[30]

In subsection A we examine the ESR spectral consequences of the MOMD and the VAR models, pinpoint typical features, and discuss spectral sensitivity to the various physical constants. In subsection B we compare our predictions with ESR results reported in the literature.

A. Theoretical Calculations. In Figure 1 we illustrate the effect of ordering and motion on the ESR spectrum which would correspond to an N–O-labeled fatty acid or phospholipid dissolved in diamagnetic phospholipid multilayers. These are the ESR

(26) Campbell, R. F.; Meirovitch, E.; Freed, J. H. *J. Phys. Chem.* **1979**, *83*, 525.
(27) DeGennes, P. G. "The Physics of Liquid Crystals"; Clarendon Press: Oxford, 1974.
(28) Berliner, L. J., Ed. "Spin-Labeling—Theory and Applications"; Academic Press: New York, 1976.
(29) Chignell, C. F.; Chignell, D. A. *Biochim. Biophys. Res. Commun.* **1975**, *62*, 136.
(30) (a) Marsh, D. "Membrane Spectroscopy"; Grell, E., Ed.; Springer-Verlag, West Berlin, 1981; (b) Marsh, D.; et al. *Biophys. J.* **1982**, *37*, 267.

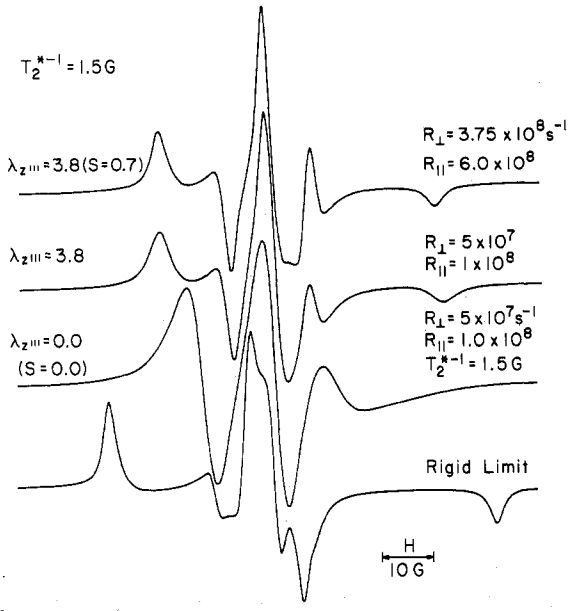

Figure 1. Typical calculated ESR spectra for the model of microscopic order but macroscopic disorder. We have used series B from Table I for the magnetic tensors ordering; z''' ordering, i.e., $z' \parallel z'''$ with $\lambda_{z'''} = 3.8$ for the upper two spectra, axially symmetric diffusion tensor with principal values $R_{y'} = R_\parallel$ and $R_{x'} = R_{y'} = R_\perp$; T_2^{*-1} is the natural line width in gauss. The third spectrum illustrates the effect of local randomness. The bottom spectrum is an isotropic rigid-lattice spectrum. The calculations were performed as described in the text.

probes commonly used in studies of model and biological membranes. A quick examination of the molecular conformation of these probes reveals that, for an extended chain, z''' is nearly parallel to the principal ordering axis z', which is also the diffusion axis. Figure 1 has been calculated for this case of the z' and z''' axes being coincident. When the lipids are fully aligned in the bilayer, their z' axes would lie along the director $\vec{d}$ corresponding to the z'' axis. The parameters entering the calculation of the spectra in Figure 1 are as follows: (a) the principal values of the hyperfine and **g** tensors which have been adopted from ref 21 obtained for labeled lipids with the nitroxide located within the chain region; (b) the dimensionless ordering potential λ which determines the extent of microscopic ordering, with $P(\theta)$, the orientational distribution function, given by[31]

$$P(\theta') = \exp[\tfrac{1}{2}\lambda(3\cos^2\theta' - 1)] \int \exp[\tfrac{1}{2}\lambda(3\cos^2\theta' - 1)] \sin\theta' \, d\theta'$$

and θ' is the polar angle defining the orientation of z' in the $x'''y'''z'''$ frame; (c) the components of the rotational diffusion tensor $R_\parallel$ and $R_\perp$ which are respectively parallel and perpendicular to z'; (d) the inhomogeneous linewidth T_2^{*-1}.

The extent of microscopic ordering is expressed by the order parameter $\langle D^2_{00} \rangle = S$ which is related to λ by means of the following expression:

$$\langle D^2_{00} \rangle \equiv S \equiv \tfrac{1}{2}\langle(3\cos^2\theta' - 1)\rangle = \int P(\theta')[\tfrac{1}{2}(3\cos^2\theta' - 1)] \sin\theta' \, d\theta'$$

Thus, each NO radical is embedded in a bilayer fragment of uniform director alignment and reorients in the presence of the local ordering potentials characterized by the director $\vec{d}$. Since we deal with a dispersion, each bilayer fragment is distributed with a random orientation in space. In practice, we first performed 10 calculations for θ (the angle between $\vec{d}$ and $\vec{B}$), ranging evenly between 0° and 90°. Basically, the calculation consists of setting up a complex symmetric matrix and diagonalizing it[22,23] to obtain

(31) Note that our definition of λ is a little different from that of ref 41. That is, $\lambda = (2/3)\lambda^{PF}$. In general, one can introduce an asymmetry term ρ into the potential (cf. ref 41) but simulations for which $\rho \neq 0$ did not appear to affect our results significantly.

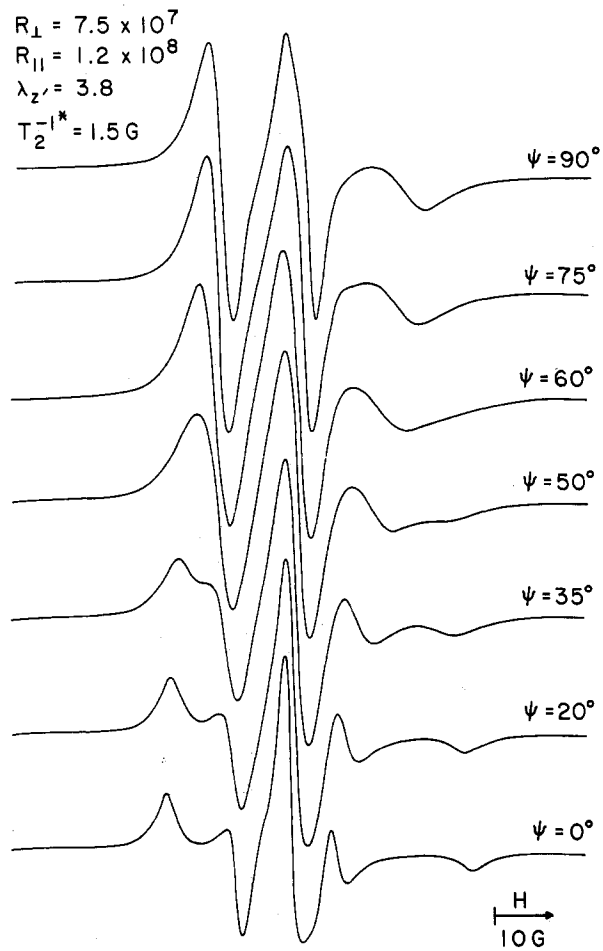

Figure 2. Calculated ESR spectra for the model of microscopic order and macroscopic disorder for different tilt angles Ψ between the diffusion axis z' and z''', the principal axis of the magnetic tensors. Values of the parameters not shown in the figure are the same as in Figure 1.

a set of eigenvalues and eigenvectors for each value of θ. These eigenvalues and vectors, for values of θ ranging from 0° to 90°, were then used to calculate intensities at different field points. The intensities thus obtained were interpolated to yield intensities at 27 values of θ (between 0° and 90°), this being found sufficient to meet with the necessary convergence requirements.

It can be seen that the top two spectra in Figure 1 have the appearance of powder-type patterns, affected mainly by the ordering, and are not very sensitive to the motional rates $R_\parallel$ and $R_\perp$. This is an outcome of the particular molecular conformation of these probes, namely $z''' \parallel z'$. Thus, care must be taken not to misinterpret such spectra as rigid limit (or immobilized spectra).[15] Their difference from a true rigid-limit (or immobilized) spectrum (shown at the bottom of Figure 1 for a macroscopically isotropic distribution) is due to the effects of motion.

We also illustrate in Figure 1 the large difference between a spectrum due to local order and macroscopic disorder from one with no local order. In Figure 2 we illustrate a different feature, namely, the effect of the tilt angle Ψ between the diffusion (and ordering) axis z' and the magnetic z''' axis. Such a tilt angle is of importance in dealing either with internal motions or with other than extended all-trans chains.

The basic assumption of the two-site model is that whenever low- and high-field peaks are visible in the spectrum in addition to a standard triplet-type nitroxide pattern (but the spectrum differs from a characteristic rigid-lattice or powder spectrum), one deals with more than a single nitroxide species. The triplet is then assumed to represent a "fluid" environment related to free lipids and the extreme peaks to belong to a true rigid-lattice component, related to nitroxides "immobilized" due to lipid–protein interactions. These are in fact *limiting* situations which might be encountered occasionally but are not typical of a liquid crys-

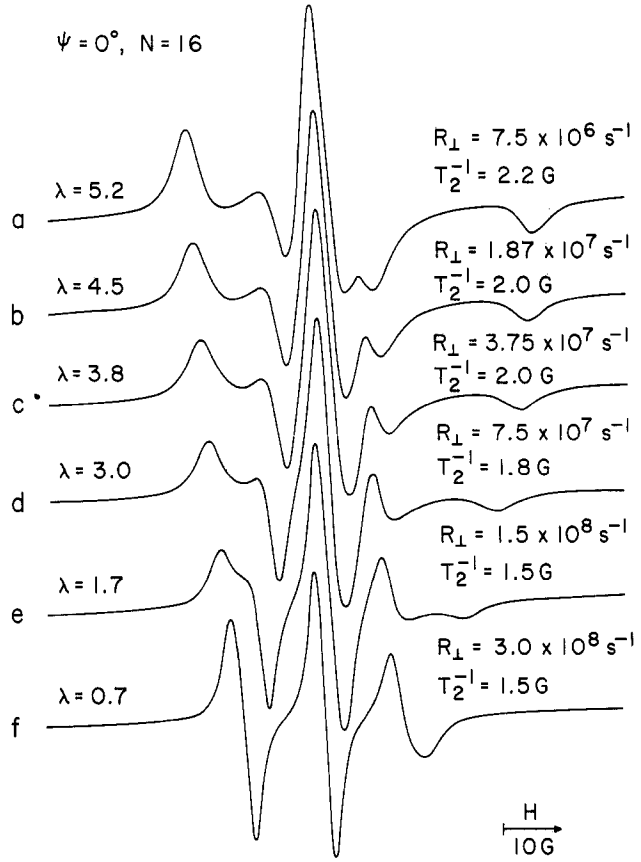

Figure 3. Spectra simulated according to the model of microscopic order–macroscopic disorder with decreasing ordering and increasing motional rates from top to bottom, illustrating typical temperature-induced spectral evolution of the ESR response from lipid dispersions doped with extended-chain doxyl nitroxides. Values of the parameters not shown in the figure are the same as in Figure 1.

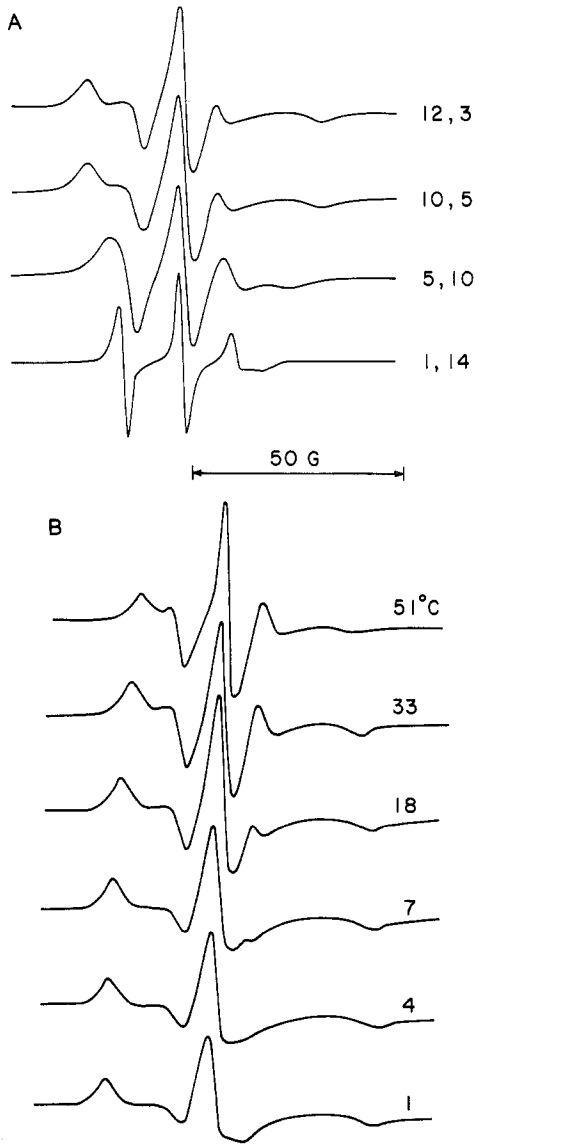

Figure 4. (A) ESR spectra of the doxylstearic acids I(m,n) (see caption for Figure 11a) in egg phosphatidylcholine randomly oriented on small glass beads (phospholipid: spin-label molar ratio 150:1) (from Griffith and Jost, 1976; Chapter 12 in ref 28). (B) ESR spectra from rabbit small intestinal brush border vesicle membranes doped with 12,3-DPPC at temperatures as denoted in the figure (from ref 19).

talline phase. That is, a triplet-type spectrum would only occur in the absence of local ordering, and a rigid (or immobilized) spectrum would only occur if *all* dynamic processes, overall and internal, were sufficiently slow on the ESR time scale ("immobilized" on the ESR time scale typically implies rotational correlation times $>10^{-6}$ s).[32] As is illustrated in Figures 1 and 2, the spectral features described above are obtained in a straightforward manner from line shape simulation based upon a physically reasonable model, viz., a single species experiencing local ordering and considerable motion (or fluidity).

The Figure 3 spectra were calculated for an extended all-trans chain conformation, viz., $z' \parallel z'''$, for increasing motional rates and decreasing order from top to bottom. It can be seen that for substantial local order ($\lambda \geq 3.8$) the line shapes have the appearance of powder patterns. The primary spectral consequences of increasing motional rates is a substantial reduction in the overall spread in field of the spectrum. For $3.0 < \lambda < 3.8$ the ESR spectrum is rather insensitive to motional rates of the order of 5.0×10^7–1.0×10^9 s^{-1}. Finally, where the ordering is low, the ESR line shape becomes sensitive to both ordering and dynamics.

These general observations can be used in deciding whether simplified models for spectral analysis are valid.

We have found that as long as $\langle D^2_{00} \rangle > 0.6$ ($\lambda > 3.0$), the ESR spectrum is similar in shape to the rigid-limit powder pattern and is determined primarily by the value of $\langle D^2_{00} \rangle$, and dynamic effects are less prominent. These are precisely the assumptions of the widely used "effective time-independent spin Hamiltonian" approach of Hubbell, McFarland, and McConnell,[33-36] which we denote as the EH model. The use of such an effective Hamiltonian is based on the assumption that (1) the motion about z', which may be described by an effective rotational diffusion tensor component $R_\parallel$ (see ref 26), is so fast that residual time-dependent effects of the averaging process, which could lead to line broadening, etc., are negligible and (2) the motion perpendicular to z', described by an effective $R_\perp$, is so slow that its effects on the spectrum are negligible. Furthermore, for such high ordering, MOMD and VAR (when the latter is being used with very slow rates $R_\perp$) also give very similar results, as both models converge essentially to an effective axially symmetric Hamiltonian. We illustrate this point by calculating spectra with the VAR model

(32) Note here that the extent to which the motion is fast or slow refers to whether there is motional averaging of the anisotropic terms in the spin Hamiltonian. One must, however, recognize that the motion is restricted in the presence of local ordering, so the range of variation of these anisotropic terms is thereby restricted. Fast motion in these cases means that there is averaging over this restricted range. Further discussion of such matters is given by Freed in ref 28, Chapter 3, as well as in ref 23, 25, and 26 and by: Polnaszek, C. F.; Bruno, G. V.; Freed, J. H. *J. Chem. Phys.* **1973**, *58*, 3185.

(33) McConnell, H. M.; McFarland, B. J. *Q. Rev. Biophys.* **1970**, *3*, 91.

(34) (a) Hubbell, W. L.; McConnell, H. M. *Proc. Natl. Acad. Sci. U.S.A.* **1969**, *63*, 16; *64*, 20. (b) Hubbell, W. L.; McConnell, H. M. *J. Am. Chem. Soc.* **1971**, *93*, 314.

(35) McFarland, B. J.; McConnell, H. M. *Proc. Natl. Acad. Sci. U.S.A.* **1971**, *68*, 1274.

(36) Knowles, P. F.; Marsh, D.; Rattle, H. W. E. "Magnetic Resonance of Biomolecules"; Wiley: New York, 1976.

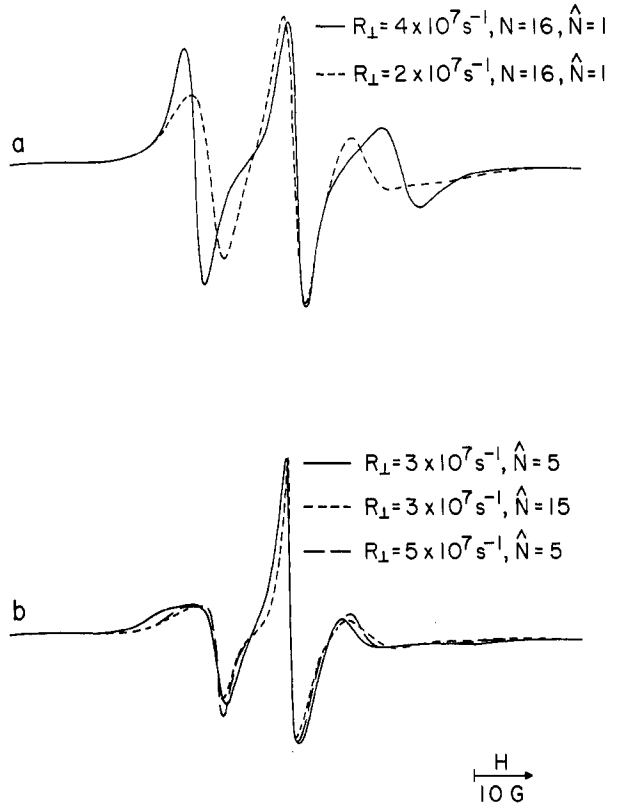

Figure 5. Calculated ESR spectra for the MOMD model illustrating the effect of the dynamical variables $R_\perp$, N, $\hat{N}$ as shown in the figure. Other parameters: (a) $\lambda = 1.4$, $\Psi = 40°$, $T_2^{*-1} = 1.2$ G. (b) $\lambda = 1.4$, $\Psi = 0°$, $N = 10$, $T_2^{*-1} = 0.4$ G. Magnetic parameters used were those in set A, Table I.

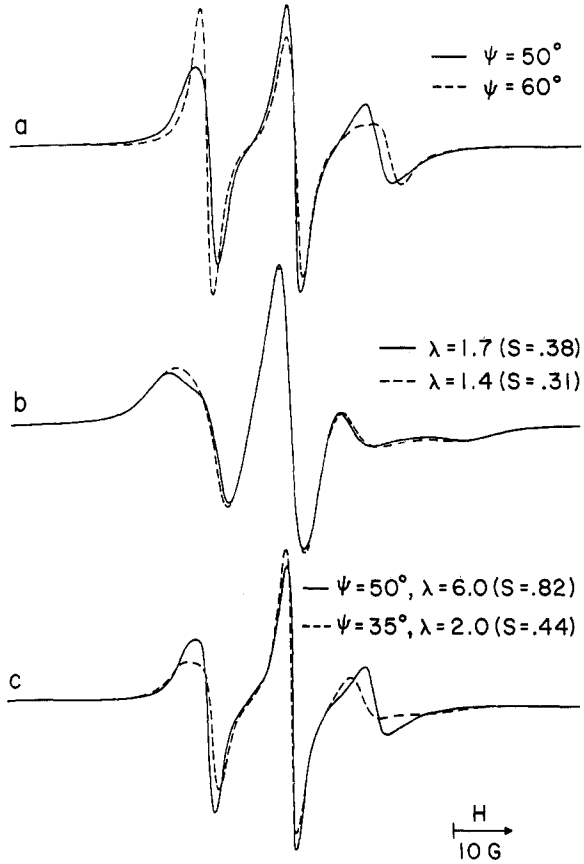

Figure 6. (a) Calculated ESR spectra for the MOMD model, illustrating the spectral effect of the "diffusion tilt", for values shown in the figure. Other parameters: set A magnetic parameters from Table I, $R_\perp = 3.0 \times 10^7$ s^{-1}, $N = 10$, $\hat{N} = 5$, $\lambda = 5.0$ ($\langle D^2_{00} \rangle = 0.78$), and $a = 1.0$ G, $b = 0.0$ for the solid line, $a = 0.7$ G, $b = 0.0$ for the dashed one. (b) Illustration of the spectral effect of local ordering for values denoted in the figure; other parameters: $R_\perp = 5.0 \times 10^7$ s^{-1}, $N = 2$, $\hat{N} = 1$, $\Psi = 0°$, $a = 1.5$ G, $b = 0$, and magnetic parameters as in Figure 9A. (c) Illustration of spectral sensitivity to combinations of ordering and "diffusion tilt" for values shown in the figure; other parameters: $R_\perp = 4.0 \times 10^7$ s^{-1}, $N = 10$, $\hat{N} = 1.0$, and $a = 0.4$ G, $b = 0.2$ G for the solid line, $a = 0.4$ G, $b = 0.25$ for the dashed one.

which are analogues of the Figure 2 spectra obtained with the MOMD approach (see below). We also refer the reader to the work of Mason et al.[25] where a particular example is considered and a detailed discussion of VAR vs. EH is outlined. Polnaszek et al.[37] have used the VAR model to analyze ESR spectra from the gel phase of dipalmitoylphosphatidylcholine (DPPC) doped with the rigid cholestane spin probe; due to the high order prevailing in this system, VAR could be used to approximate the MOMD model (although accurate simulations would require the full theory[24]). (The VAR model was also used to analyze ESR spectra from spin-probe-doped mitochondrial membrane lipids of the brown adipose tissue of cold-adapted rats and hamsters[20] although its applicability was not clearly established.)

For lower ordering and/or faster motions, EH is not applicable, as the motional effects severely modify the ESR line shape. When this simple model is used, erroneous estimates of the order parameter are obtained, as demonstrated by Mason et al.[25] Moreover, information on motional rates and chain conformation (the latter related directly to the value of the diffusion–tilt angles Ψ and ϕ, to which the ESR spectra are, as shown in Figures 2 and 3, extremely sensitive) would be totally lost.

These general considerations should be kept in mind while analyzing experimental ESR spectra. We present in Figure 4A ESR spectra obtained from egg phosphatidylcholine doped with various NO-labeled stearic acid spin probes [denoted as (m,n), with the NO label attached at the $n + 2$ carbon atom counting from the carbonyl carbon, exclusively and $n + m = 15$]. Comparison with Figures 1 and 3 indicates that for the 12,3 probe this model may be valid as a first approximation, whereas for probes with the NO group further removed from the carbonyl group, the MOMD model should be used. In Figure 4B we show ESR spectra from rabbit small intestinal brush border vesicle membranes doped with (12,3) DPPC.[19] On studying the trends in Figure 3, and comparing these spectra with the experimental spectra of Figure 4, A and B, we conclude that the spectra of Figure 4A show incipient slow motion and moderate or low ordering. Consistent with our expectations, we find that as the position of the nitroxide moiety is shifted to the lower and more flexible parts of the stearic acid chain (n increasing in Figure 4A), the motion gets more and more rapid and the ordering decreases. When the ordering is low, the spectra are quite sensitive to changes in the order parameter λ (Figure 3d–f).

In contrast, the spectra of Figure 4B show slower motion and higher ordering and resemble the spectra calculated on the basis of the VAR model. In either case, moderate ordering and incipient slow rotational motion are implied, and therefore the EH model is likely to be approximately valid in this temperature range. (This is a typical example where the single-site interpretation is supported by the observation that pure lipids and protein-containing lipids give rise to very similar ESR spectra, implying homogeneity of the membranes—see Figure 1 in ref 19.)

We further detail the spectral sensitivity to the various physical constants in Figures 5–10. The sensitivity of the ESR spectra to changes in ordering can be seen in Figure 3. We find that the spectra are most sensitive to changes in λ when λ is small (low ordering). For moderate ordering, when λ lies in the range $3 \leq \lambda \leq 3.8$ the spectra change less markedly, whereas when the ordering is higher ($\lambda \geq 4.5$) there is very little change in the spectra. On the other hand, widely differing ESR line shapes are obtained by varying the diffusion tilt Ψ, as shown in Figure 6a.

(37) Polnaszek, C. F.; Marsh, D.; Smith, I. C. P. *J. Magn. Reson. 43*, **1981**, 54.

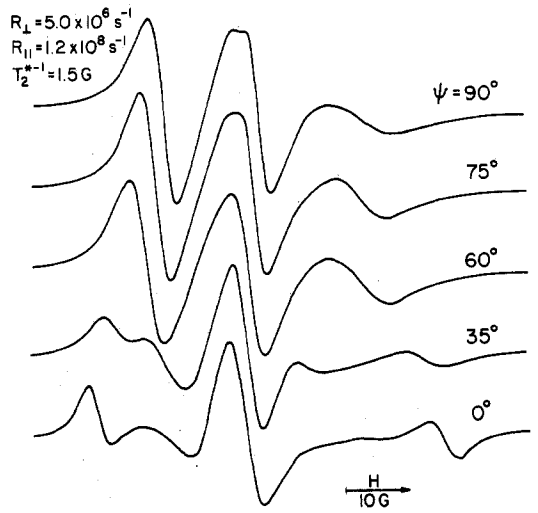

Figure 7. Calculated ESR spectra for the model of very anisotropic reorientation for different tilt angles Ψ between the diffusion axis z' and z''', the principal axis of the magnetic tensors. We have used series A from Table I for the magnetic tensors, and all other parameters employed are given in the figure.

Also, the ESR spectrum is rather sensitive to changes in the dynamic variables, as shown by the considerable differences in the two traces in Figure 5a, brought about by increasing $R_\perp$ from $2 \times 10^7\ s^{-1}$ for the dashed line to $4.0 \times 10^7\ s^{-1}$ for the solid one. This point is further illustrated in Figure 5b, where rather big spectral alterations arise from changes in $R_\perp$, and $\hat{N}$, both related to the diffusion tensor. [$N = R_\parallel/R_\perp$ ($\hat{N} = \hat{R}_\parallel/\hat{R}_\perp$) and the diffusion rates $R_\parallel$ and $R_\perp$ ($\hat{R}_\parallel$ and $\hat{R}_\perp$) denote the principal values of the diffusion tensor which is diagonal in the molecular (director) frame.] The spectra are less sensitive to changes in N.

For lower ordering and/or nonzero diffusion tilt, the ESR spectra are very sensitive to all the physical constants. The dramatic spectral consequences of decreasing $R_\perp$ from 2.0×10^7 s^{-1} (solid line) to $4.0 \times 10^7\ s^{-1}$ (dashed line) with $\Psi = 40°$ (Figure 5a), increasing Ψ from 50° to 60° (Figure 6a), changing λ (Figure 6b), or varying both and simultaneously (Figure 6c) all confirm this statement.

In Figure 7 we show ESR spectra calculated with the VAR formulation for various angles Ψ. The input variables used to obtain the Figure 7 line shapes are similar to those employed to compute the Figure 2 spectra with the MOMD model. Although the corresponding spectra in Figures 2 and 7 differ, gross features are similar, and the trends observed upon varying Ψ are common to both series. This is expected, as noted above, for high ordering. It indicates the extent to which VAR can be used as an approximation to MOMD.

With this in mind, we present in Figure 8A–D series of ESR spectra calculated with the VAR model for various angles Ψ and

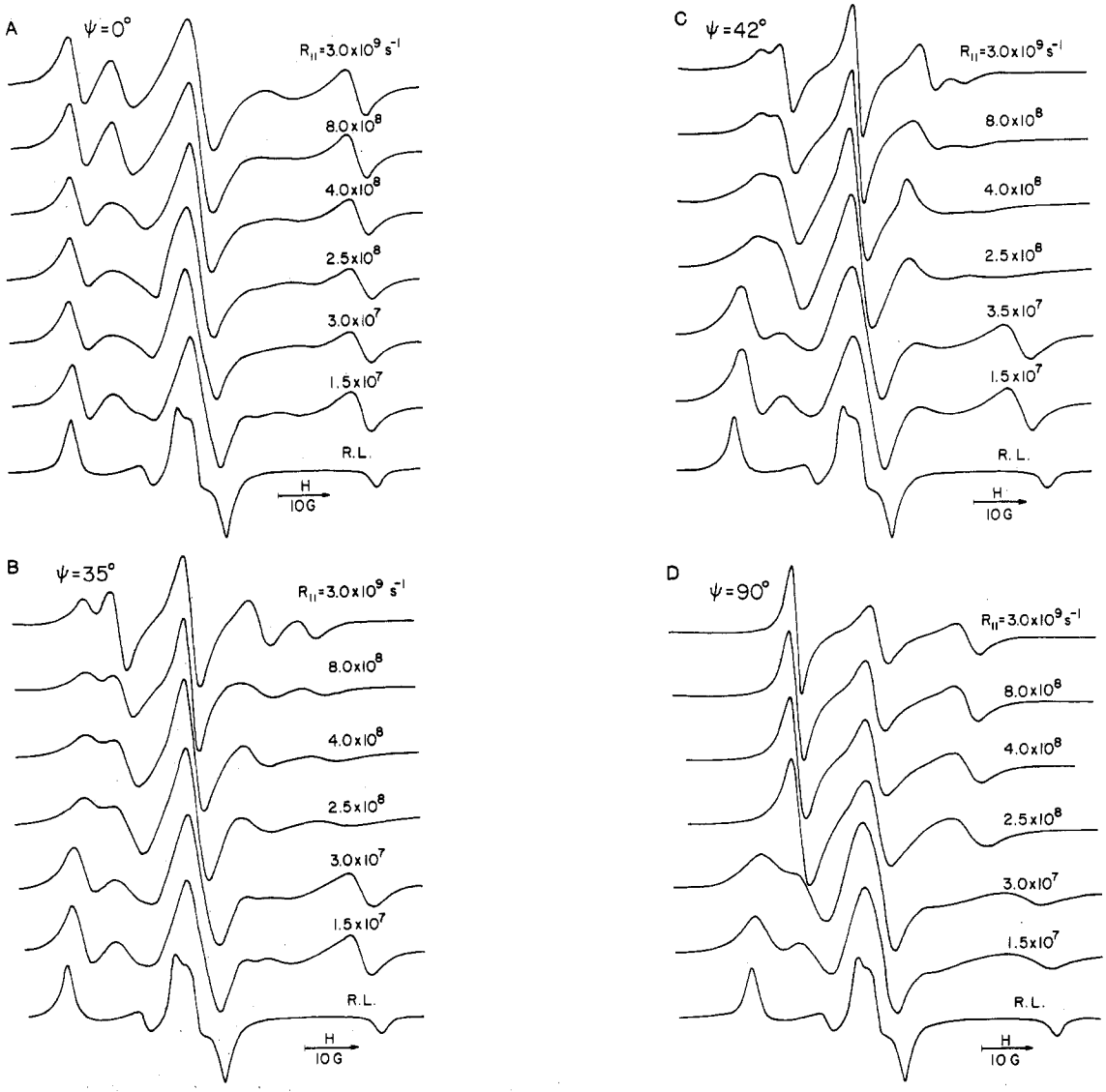

Figure 8. Calculated ESR spectra for the VAR model with the set A magnetic parameters from Table I, $R_\perp = 5 \times 10^6\ s^{-1}$, $a = 1.5$ G and (A) $\Psi = 0°$, (B) $\Psi = 35°$, (C) $\Psi = 42°$, (D) $\Psi = 90°$, for varying motional rates $R_\parallel$, as denoted in the figure.

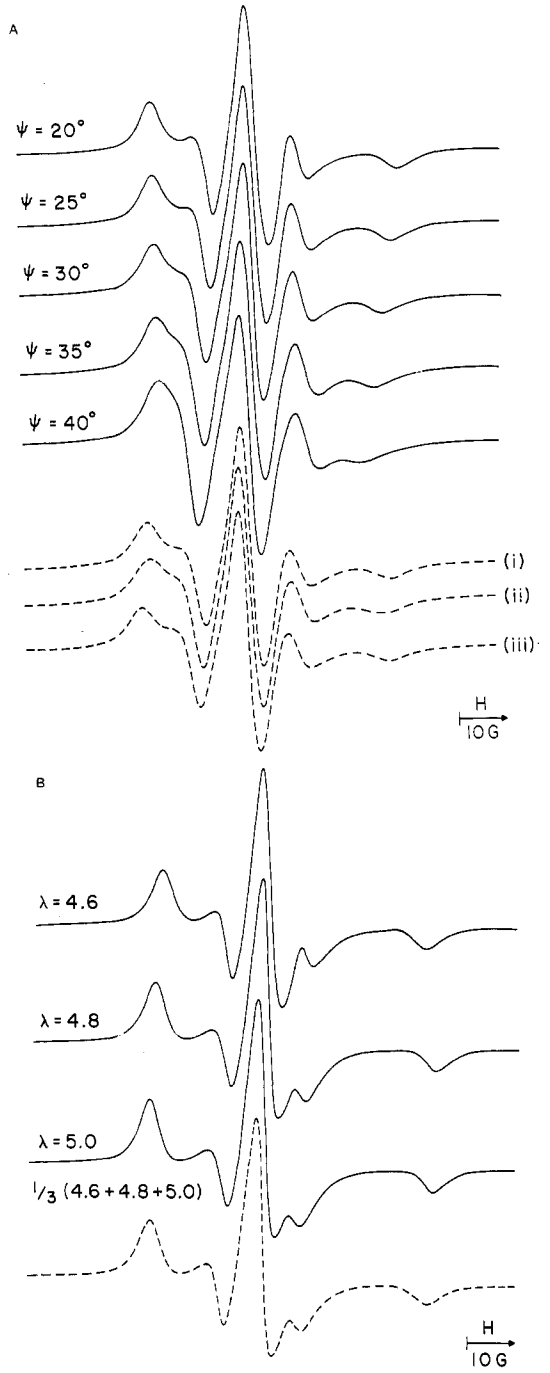

Figure 9. (A) ESR spectra calculated by using the MOMD model illustrating the effect of superimposing spectra with varying diffusion tilt angle, Ψ, as shown in the figure. Other parameters: $R_\perp = 1 \times 10^8$ s^{-1}, $N = 2.4$, $\hat{N} = 1.0$, $\lambda = 4.5$. $a = 2.0$ G, $b = 0$ G, where $T_2^{*-1} = a + b \cos^2 \theta$ (see text). Magnetic parameters used were those of set A, Table I. The dashed curves are the results of superimposing spectra varying in the tilt angle Ψ using (i) a simple average of 20°, 25°, 30°, (ii) a Gaussian average centered at $\Psi = 30°$ with $\sigma = 1°$, (iii) a Gaussian average centered at $\Psi = 30°$ with $\sigma = 10°$. (B) Ordering as shown in the figure. Other parameters: $N = 16$, $\Psi = 0$, $\hat{N} = 1.0$, $a = 2.0$ G, $b = 0$; (i) $R_\perp = 1.4 \times 10^7$ s^{-1} ($\lambda = 4.6$), (ii) $R_\perp = 1.1 \times 10^7$ s^{-1} ($\lambda = 4.8$), (iii) $R_\perp = 0.9 \times 10^7$ s^{-1} ($\lambda = 5.0$). Magnetic parameters used were those of set A, Table I. The dashed curve shown at the bottom is obtained from the average of the traces corresponding to $\lambda = 4.6$, 4.8, 5.0.

motional rates $R_\perp$ and $R_\parallel$. A typical inhomogeneous line width T_2^{*-1} of 1.5 G was used, $R_\parallel$ was varied between extreme values (from the motional narrowing limit down to the rigid limit), and $R_\perp$ was chosen to be 5.0×10^6 s^{-1}, which is close to, but not identical with, the rigid-limit value.

With chemically labeled proteins, VAR is an appropriate model for analyzing dramatic effects on the ESR spectra. Recall that at room temperature the rate for Brownian reorientation of particles with a molecular weight of roughly 5×10^5–10^6 au is of the order of 5×10^6–10^6 s^{-1}, i.e., slow on the ESR time scale. Motional averaging, if any, is therefore likely to be mainly due to internal modes of reorientation, and if one can assume a mean diffusion axis z' for segmental motion, comparison of experimental spectra with calculated line shapes of the type illustrated in Figure 8A–8D permits one to estimate the tilt angle between z' and the NO bond. Also, $R_\perp$, representing the overall Brownian reorientation of the macromolecular complex as well as $R_\parallel$, representing the segmental motion, can, in general, be determined (if they are not too slow).

B. Comparison with Experiment. There are two distinct ways in which the behavior of the lipids is studied: (i) One varies the position of the nitroxide moiety along the lipid chain. This is the approach followed, for example, by Chignell and Chignell,[29] who have investigated the purple membrane from *Halobacterium halobium* by doping it with various nitroxide-labeled stearic acids. Such studies would lead to information concerning the relative flexibilities of different parts of the chain. (ii) One labels the lipid at *a* particular site and adds varying amounts of protein to the pure lipid system.[2,30] These experiments probe the molecular dynamics at the nitroxide site as a function of protein concentration. Of course, in doing such experiments, one must choose the position of the nitroxide label judiciously—that is, one labels that part of the chain which is most sensitive to changes in the surrounding medium.

We focus on the two above-mentioned cases separately.

The experimental spectra of Chignell and Chignell are shown in Figure 11A. Since the purple membrane from *Halobacterium halobium* is rather rigid, one finds that when the nitroxide moiety is close to the carboxylic end of the stearic acid label, the spectra are almost temperature invariant and near rigid-limit-like in appearance. As the position of the nitroxide is moved further down the chain, the spectra are found to show motional effects and are no longer temperature invariant. In fact, one finds from Figure 11A(iii) that when the nitroxide moiety is near the end of the chain [stearic acid label (1,14)], the spectra at 5° and 25° are widely different.

On comparing these spectra with our calculated spectra, we find that the spectra from the 12,3 stearic acid are very similar to those obtained from the VAR model, in keeping with the high ordering and very anisotropic motion of the probe. With 5,10 stearic acid the spectra are broader and display a smaller anisotropy, consistent with the expected lower ordering and higher mobility upon progressing toward the methyl end. Finally, with 1,14 stearic acid, where the nitroxide moiety is at the most flexible part of the chain and therefore most sensitive to environmental effects, we find that the spectra change quite dramatically with temperature. The line shapes obtained are also indicative of reduced ordering and smaller anisotropy.

On examining the spectra for the stearic acid probe (Figure 11A), as well as those in Figure 4, A and B, we note that though these spectra show the same qualitative features as those predicted by the MOMD model, the low-field peak arising from $\theta = 0°$ is invariably more diffuse in character than that calculated from the model. In order to "explain" this behavior, one might invoke an angular-dependent inhomogeneous broadening contribution arising from the superhyperfine structure due to the protons adjacent to the NO moiety. Such an inhomogeneous line width would have the form

$$T_2^{*-1} = T_{2,0}^{*-1} + T_{2,2}^{*-1} \cos^2 \theta$$

where θ is the polar angle that the spin probe molecule makes with the laboratory frame. The contribution due to $T_{2,2}^{*-1}$ arises, for example, from the angular dependence of the adjacent protons.[38] We found that the fit between theory and experiment could be improved considerably in this manner. However, values of $T_{2,2}^{*-1}$ that are larger than $T_{2,0}^{*-1}$ are unphysical (although they may compensate for the limitations of our simple models of motional

(38) Polnaszek, C. F.; Freed, J. H. *J. Phys. Chem.* **1975**, *79*, 2283.

dynamics in oriented media[39]), so we therefore seek alternative mechanisms that might account for the desired broadening.

We generalize the model of microscopic order and macroscopic disorder as follows: We postulate that the microscopically ordered domains exhibit some randomness in their precise properties due to local variations in the lipid bilayer and/or the effects of the proteins. This yields some microscopic disorder. The implications of this are discussed below.

(*i*) *Parameters Pertaining to the Conformation of the Probe.* Referring to Figure 12, one finds that the probe geometry can be characterized by two parameters: the ratio of the diffusion coefficients parallel and perpendicular to the long axis of the molecule (i.e., N), and the diffusion tilt angle Ψ which is indicative of a kink along the chain (Figure 12b). One may expect a distribution of kinks throughout the bilayers. We represent this by a distribution of values of Ψ and/or N; e.g., a more extended chain will lead to a decrease in Ψ and/or an increase in N.

To simulate the effect of a distribution in the arrangement of the chains, we have superimposed spectra in which Ψ is slightly different. Since we find from Figure 2 that our spectra are highly sensitive to the diffusion tilt angle Ψ, we expect that such a superposition will lead to a broadening of the low-field peak. The results of these simulations are shown in Figure 9A.

(*ii*) *Parameters Pertaining to the Dynamics of the Probe.* We have also calculated spectra in which the fluidity and ordering of the probe differ from one region to another by combining spectra in which the rotational correlation times and the order parameters vary over a range. It is found that when the ordering is high, the spectra are quite insensitive to changes in motional rates and/or ordering. Such superpositions, therefore, did not show any interesting effects (Figure 9B), though they might have important implications for lower ordering when the ESR spectra are sensitive to all the parameters.

It is clear that both mechanisms i and ii outlined above lead to a broadening of the low-field peak relative to the single spectra.

In a recent study of 1,14 stearic acid probe in a thermotropic smectic liquid crystal,[23c] we found that allowing for an anisotropy in the viscosity (i.e., $\hat{N} > 1$) significantly improved the fits to the *well-oriented* spectra. We therefore considered its effects in the present case, and typical simulations are illustrated in Figure 10. Figure 10, i and ii, show respectively the effect of anisotropic viscosity on spectra at $\theta = 0°$ and 90°. It is clear that the $\theta = 0°$ spectrum is far more sensitive to anisotropic viscosity than the $\theta = 90°$ spectrum; we find that increasing the value of $\hat{N}$ broadens the outer lines for $\theta = 0°$ but has practically no effect on the $\theta = 90°$ spectrum. Given that this has the same effect as arbitrarily adding a $T_{2,2}^{*-1}$, but appears justified as a result of the previous work on oriented smectics,[24] we have used an $\hat{N} > 1$ in simulating the protein–lipid spectrum as shown in Figure 11B. Figure 10iii shows the influence of anisotropic viscosity on a composite spectrum calculated with the same parameters as in i and ii using the MOMD model. As expected, we find that the low-field peak arising from $\theta = 0°$ is more affected than the low-field peak due to $\theta = 90°$, bringing the simulation into closer correspondence with observation.

In Figure 11B we show ESR spectra at 50 °C of 2% (w/w) phospholipid spin probe DPPC gramicidin A dispersion at lipid/protein ratios corresponding to 1:1 and the pure lipid. Along with these, we have also shown our best simulations using the MOMD model. The agreement seems quite reasonable. We note, however, that our best fits to the experimental spectra using the MOMD model were achieved for moderate to high lipid to GA ratios (e.g., 10:1 and higher) and for very low ratios (e.g., 1:1). While the intermediate region was not fit as satisfactorily, the small spectral features required in this region could be influenced by finer details of the simulations.

In commenting on the uniqueness and accuracy of the various physical constants as determined by line shape simulations, we note that within the dynamic range under consideration, spectral sensitivity is highest to variations in the diffusion tilt angle but

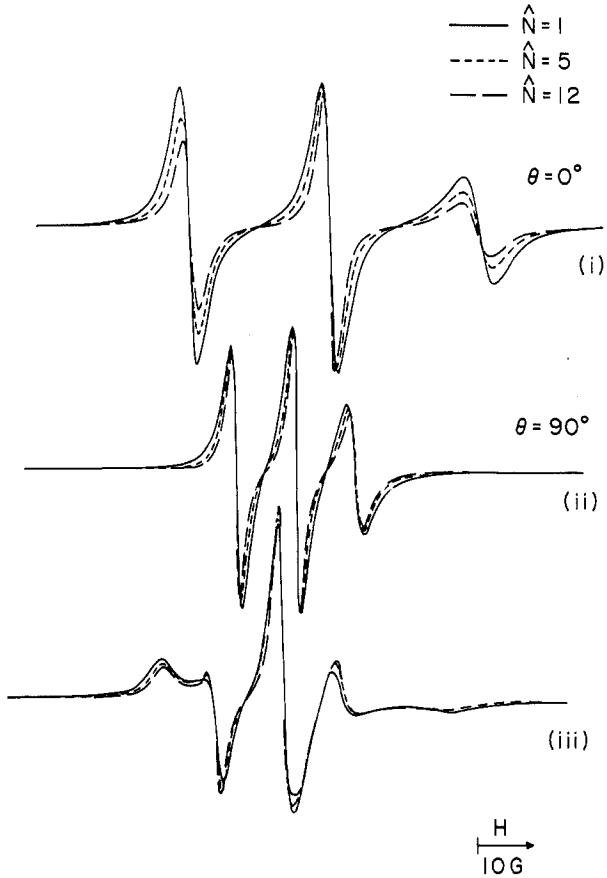

Figure 10. Effect of anisotropic viscosity on ESR spectra. Magnetic parameters as in set A Table I. Other parameters: $R_\perp = 7 \times 10^7\ s^{-1}$, $N = 10$, $\lambda = 2.2$, $a = 1.0$ G, $b = 0$ where $T_2^{*-1} = a + b\cos^2\theta$, θ being the angle between the local director and the lab fixed (mean) director: (i) for a fixed value of $\theta = 0°$, (ii) for a fixed value of $\theta = 90°$, (iii) ESR spectra calculated by using the MOMD model for values of $\hat{N}$ as indicated in the figure.

is moderate for changes in $R_\perp$ and $\hat{N}$, i.e., parameters associated with the diffusion tensor, and is relatively low for alteration in the local ordering and N, as discussed previously.

We find that $\Psi = 20°$ is best to fit the 1:1 mixture (Figure 11B). Since $\Psi = 0°$ would correspond to an alkyl chain with an extended all-trans conformation, then $\Psi \neq 0$ would imply that the chain is deformed at the position of the NO label. We illustrate in Figure 12 a possible deformation of a double kink adjacent to the NO label which would introduce a 20° tilt.[40] Thus, a value of $\Psi = 20°$ could correspond to a mean conformation including a long-lived kink distorting the chain segment attached to the nitroxide group from an all-trans conformation, as well as some other type(s) of deformations.

Further, our analysis leads to the result that the motional rate $R_\perp$ increases from $4 \times 10^7\ s^{-1}$ for the 1:1 mixture to $1.4 \times 10^8\ s^{-1}$ for the pure lipid. The latter value is of the same magnitude as that seen in the spectra of long-chain fatty acids in low water content lyotropic mesophases.[21] The significant difference in rotational diffusion times between the protein–lipid mixture and the pure lipid strongly suggests that the rotational relaxation of the nitroxide moiety is of the surrounding protein molecules. The value of $\Psi = 0°$ and $N = 16$ for the pure lipid would suggest an all-trans chain geometry. The addition of the protein molecule to the lipid results in a deformation of this conformation ($\Psi = 20°$, $N = 10$). The value $\hat{N} = 5$, showing that anisotropic viscosity develops as the protein is added, is interpreted as a deviation from simple Brownian reorientation (e.g., slowly relaxing local structure).[38,41,42]

(39) Freed, J. H. *J. Chem. Phys.* **1977**, *66*, 4183.

(40) Lee, T. D.; Birrell, B.; Fjorkman, R. J.; Keana, J. F. W. *Biochim. Biophys. Acta* **1979**, *550*, 369.

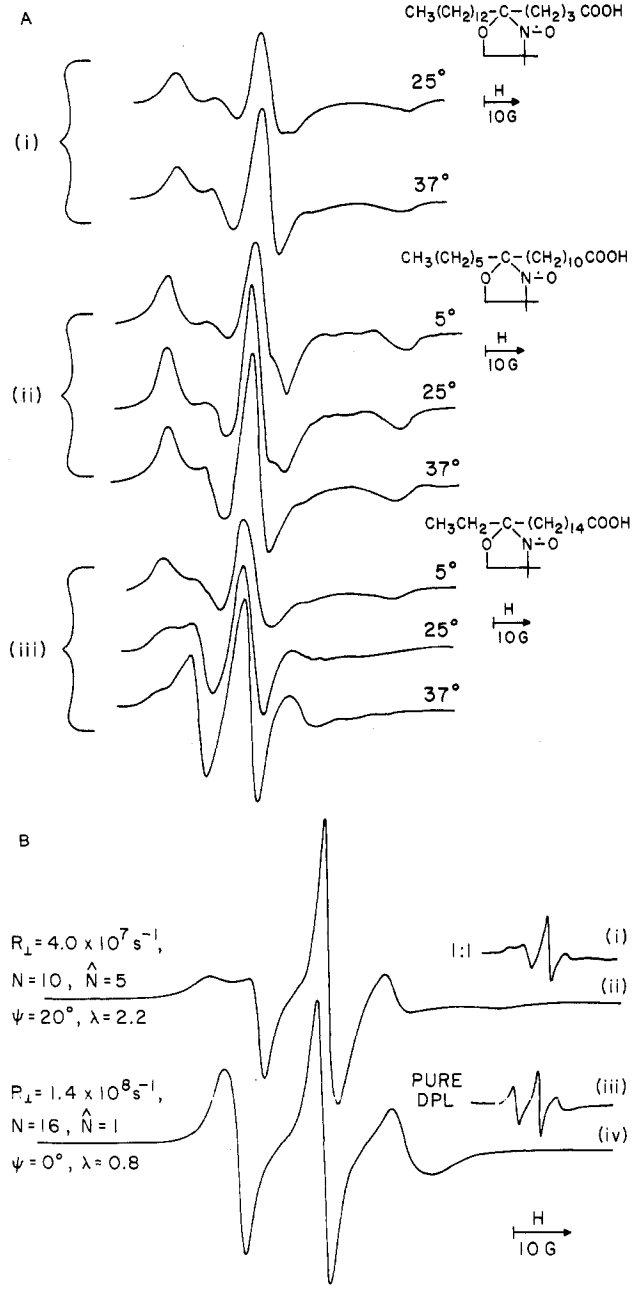

Figure 11. (A) ESR spectra of stearic acid label I(m,n) (2×10^{-5} M) bound to purple membranes (1.2 mg/mL) from *Halobacterium halobium* at the temperatures indicated in the figures

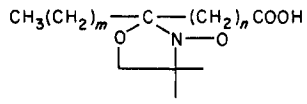

I(m,n)

(i) m = 12, n = 3; (ii) m = 5, n = 10; (iii) m = 1, n = 14 (from ref 29). (B) (i, iii) ESR spectra at 50 °C of 2% (w/w) phospholipid spin probe in dipalmitoylphosphatidylcholine gramicidin A dispersion with the indicated molar ratios. Reproduced from ref 2. (ii, iv) ESR spectra calculated from the MOMD model using the parameters as shown in the figure. Magnetic parameters used were those from set A of Table I. In ii, $T_2^{*-1} = a + b\cos^2\theta$, with a = 0.5 G, b = 0.2 G. In iv, a = 1.0 G, b = 0 G.

The local ordering was found to be low ($0.8 < \lambda < 2.2$). This shows that a high degree of flexiblity exists in the end-labeled

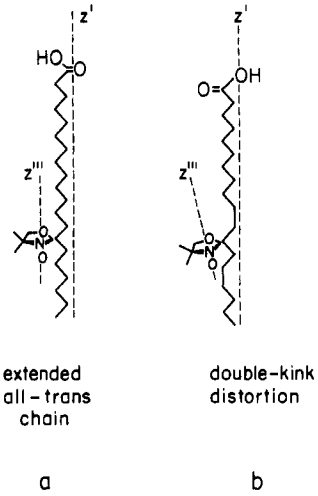

Figure 12. (a) Schematic drawing of a fully extended all-trans chain configuration of an oxazolidine nitroxide labeled fatty acid, where z''' is approximately parallel to z'. (b) Schematic drawing of an alkyl chain with two kink distortions flanking the nitroxide-bearing carbon atom, where z''' is tilted by approximately 20° relative to z', following Lee et al.[40]

position of the lipids. As the concentration of the protein is increased, the molecules of lipid are squeezed more tightly, accounting for the decrease in motion and increase in ordering.

Although the fit between theory and experiment is not perfect, the spectral sensitivity illustrated in Figures 1–3 and 5–10 clearly shows that one can expect to fit the motional and ordering parameters with reasonable confidence.

In particular, our results for the one-site model suggest that the addition of a protein to the pure lipid has the following effects. The lipid molecules experience overall increased microscopic order, decreased motional rates, and possibly chain distortion. This is distinct from the two-site model, wherein molecules of lipid in the near vicinity of the protein are significantly immobilized compared to the bulk lipids and any effects of local ordering are largely ignored. In the two-site model, addition of protein primarily increases the number of immobilized lipids, but in the one-site model all lipids are similarly (though not necessarily identically) affected.

The last example that we present in Figure 13 relates to ESR spectra obtained from the ATPase enzyme of the sarcoplasmic reticulum (SR) membrane labeled selectively with a nitroxide free radical.[12] Using the *N*-(1-oxy-2,2,6,6-tetramethyl-4-piperidinyl)iodoacetamide spin probe (ISL) as precursor for the paramagnetic complex, 1 mol of spin-label reacted per one molecular weight 1 000 000 ATPase chain, indicating only one sulfhydryl residue on the enzyme had been labeled. ESR spectra from the NO-labeled membrane-enzyme under various conditions (a) plain SR (no substrate), (b) with AMP-P(NH)P (adenyl-5-yl imidodiphopshate), and (c) AMP-P(NH)P + Ca^{2+}) are shown in Figure 13a. The ISL-SR spectra have been characterized in previous studies[11,13,14] as composite two-component patterns consisting of a "mobile" and an "immobile" component, denoted in Figure 13a by A and B, respectively.

By inspection of Figures 7 and 8, we find that one may define a mean internal diffusion axis z' tilted at approximately 30–45° from the NO π-orbital, with $R_\perp$ of the order of 5.0×10^6 and $R_\parallel$ somewhat higher than $10^8\ s^{-1}$. Interestingly, very similar spectra were obtained with poly(benzyl glutamate) (PBLG) polymers end-labeled with a six-membered piperidine ring in dimethylformamide solutions, illustrated in Figure 13b. These spectra were carefully analyzed by Mason et al.[25] using the VAR model and the best-fit calculated spectra, corresponding to the experimental Figure 13b line shapes, are shown in Figure 13c. The parameters used to obtain the Figure 13c spectra were Ψ =

(41) Lin, W. J.; Freed, J. H. *J. Phys. Chem.* **1979**, *83*, 379.
(42) Broido, M. S.; Meirovitch, E. *J. Phys. Chem.* **1983**, *87*, 1635.
(43) Fisher, T. H.; Levy, G. C. *Chem. Phys. Lipids* **1981**, *28*, 7.
(44) Alonso, A.; Restall, C. J.; Turner, M.; Gomez-Fernandez, J. C.; Goni, F. M.; Chapman, D. *Biochim. Biophys. Acta* **1982**, *689*, 283.

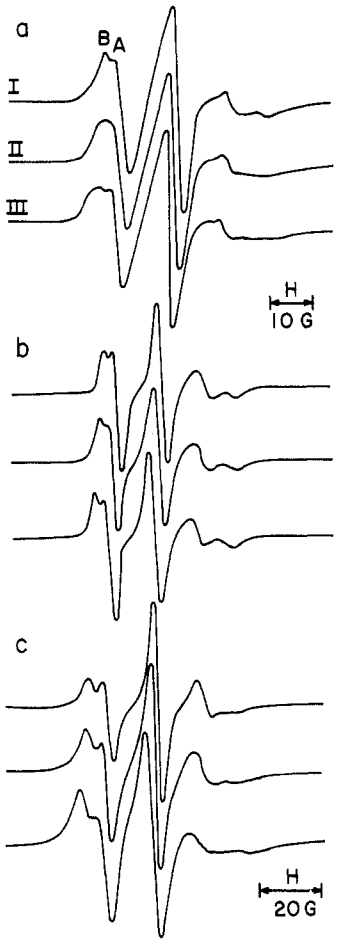

Figure 13. (a) ESR spectra of ISL-SR (I) in buffer 20 mM 4-morpholinepropanesulfonate, pH 6.8, 80 mM KCl, and 5 mM $MgCl_2$; (II) with 5 mM AMP-P(NH)P (adenyl-5'-yl imidodiphosphate and 1 mM EGTA (ethylene glycol bis(β-aminoethyl ether)-*N,N,N',N'*-tetraacetate; (III) with 5 mM AMP-P(NH)P and 5 mM $CaCl_2$. All spectra were measured at 25 °C. A and B denote the presumably "mobile" and "immobilized" components, respectively, of the two-site model (ref 12). (b) ESR spectra of poly(benzyl glutamate) labeled with 2,2,6,6-tetramethyl-4-aminopiperidine-1-oxyl in dimethylformamide at room temperature.[25] The polymer concentration (volume fraction) was (I) 0.128, (II) 0.148, and (III) 0.2. (c) Calculated spectra with the magnetic parameters of the doxyl spin-label where $a_{z'''} = 30.8$ G, $a_{x'''} = a_{y'''} = 5.8$ G, $g_{x'''} = 2.0089$, $g_{y'''} = 2.0058$, and $g_{z'''} = 2.0021$.[34] Other parameters: $\Psi = 41.7°$, $R_\perp = 3.3 \times 10^6$ s^{-1}, $R_\parallel = 8.33 \times 10^8$, 4.17×10^8, and 2.5×10^8 s^{-1}, respectively, from top to bottom.[25]

41.7°, $R_\perp = 3.3 \times 10^6$ s^{-1}, and $R_\parallel$ equal to 8.33×10^8, 4.17×10^8, and 2.5×10^8 s^{-1}, respectively, from top to bottom. The diffusion tilt Ψ was interpretated in terms of coincidence of z' and the NH–CH bond, implying that the viscosity-induced changes in the ESR spectra from end-labeled PBLG are due solely to variations in the rate of spinning about the NH–CH bond.

In complete analogy, the piperidine ring attached to the ATPase enzyme through the NH–CH bond rotates about the latter. Then the similarity in the two sets of experimental spectra suggests that $R_\perp$, $R_\parallel$, and Ψ are very similar to those used to calculate the Figure 13c spectra. The spectral consequence of adding the substrate AMP-P(NH)P and Ca^{2+} to the pure ISL-SR complex can be thus interpreted on a molecular basis in terms of an increase in the rate $R_\parallel$ for segmental motion from roughly 4×10^8 s^{-1} to approximately 8×10^8 s^{-1}. When AMP-P(NH)P alone is added, the inhomogeneous line width T_2^{*-1} apparently becomes somewhat broader, decreasing spectral resolution. It should be pointed out, however, that uniqueness and accuracy can, in general, be enhanced by simulating series of ESR spectra, whereby a considerable range of the dynamic timescale is spanned (as was the case with the NO-labeled PBLG), rather than relying on a single spectrum. For the particular case of the ISL-SR complex, we could rely on similarity with the PBLG spectra to extract information from the Figure 13a spectra.

IV. Further Discussion and Summary

We have seen that the spectral change from an isotropic three-line spectrum to one with additional splittings can be induced by increasing the local order (and reducing the motional rates), while the prominence of the additional splitting is diminished by $\Psi \neq 0°$. A model explaining the spectral modifications induced by adding proteins to lipid dispersions emerges from our results, if we assume the proteins increase the microscopic ordering, reduce fluidity, and also induce distortions in the chains of the boundary lipids. Such effects could then be transmitted to the other lipids, so that the whole lipid phase senses these changes. The chain distortions would mean that they are, in effect, being ordered at an angle tilted relative to their local principal axis system represented by the magnetic tensor principal axes. One may further conjecture that there would be fluctuations in both ordering and Ψ as the proteins reorient and the lipids are forced to readjust their alignment, but these could be slow on the ESR time scale. The ESR spectra which we have calculated suggest that such fluctuations, albeit static on the ESR time scale, could be of some importance in explaining some of the more subtle aspects of the line shapes. We now wish to discuss some further implications of this model.

A. Why Spectra Based on the MOMD Model Can Have the Appearance of a Two-Site Model. Recent ESR studies based upon the two-site model employ spectral subtraction to elucidate the two (or more) "component" spectra (e.g., ref 45 and 46 and references therein). We now wish to address the question: Why is it that a one-site model can satisfactorily reproduce spectral features that intuitively appear to arise from two (or more) component spectra? The main point here is that the macroscopic disorder of the dispersion implies an *averaging* of *different* spectra obtained for each orientation of the director $\hat{d}$ with respect to the external magnetic field B. As we have already pointed out, for each angle θ, a different spectrum is obtained provided there is appreciable ordering.[21] As is well-known, derivative polycrystalline ESR spectra when averaged over the unit sphere are dominated by the contributions from $\theta = 90°$ and 0° (cf. Figure 1).[49] In the present case, the appearance of the averaged spectra will be influenced by (i) the extent of ordering, by (ii) a tilt angle $\Psi \neq 0°$, and by (iii) (slow)-motional effects, leading to the detailed differences that we have observed in the simulations. Thus, it is possible that a spectral subtraction technique could be used with some *apparent* effectiveness even when a one-site model, such as we are proposing, is appropriate. Preliminary efforts at using our theoretically generated spectra for spectral subtraction have met with some success and provide further support for the relevance of our model.

B. NMR Predictions. We now wish to make a few comments about NMR predictions in the context of our single phase model. In the usual NMR results, one observes for the membranes with protein that (i) quadrupole splitting decreases slightly, (ii) the ^2H T_1 values are a little shorter, and (iii) the apparent line widths increase.[16] The decrease in quadrupole splitting would be explained as an increase in angle Ψ, representing the effect of tilting the chain due to induced distortions by the proteins, consistent with a suggestion of Seelig and Seelig.[16] The shortening of T_1 values could correspond to a decrease in the rotational diffusion

(45) Brotherus, J. R.; Griffith, O. H.; Brotherus, M. O.; Jost, P. C.; Silvius, J. R.; Hokin, L. E. *Biochemistry* **1981**, *20*, 5261.

(46) Watts, A.; Davoust, J.; Marsh, D.; Devaux, P. F. *Biochim. Biophys. Acta* **1981**, *643*, 673.

(47) A relatively slow modulation of the angle of tilt Ψ would lead to an additional contribution to T_1^{-1} (and T_2^{-1}) which would be akin to the model of a slowly relaxing local structure introduced by Polnaszek and Freed (1975) to explain local motions of probes in liquid crystalline media.

(48) Meirovitch, E.; Freed, J. H. *Chem. Phys. Lett.* **1979**, *64*, 311.

(49) This statement is also true in the limit of strong ordering and rapid motions, because in this limit one gets spectra as a function of θ from quasi-static partially averaged axial magnetic tensors along the principal axis of diffusion.

rate (primarily about the tilted axis of ordering), i.e., an increased microviscosity (see, e.g., Seelig and Seelig[16,47]). The broadening of the spectral lines can be due either to slow-motional effects[48] or to a distribution of order parameters.[16] Slow-motional effects are, in our model, consistent with decreasing $R_\parallel$ (and $R_\perp$), while a distribution of observed order parameters would result if there is some variation in Ψ because of a distribution in the number and types of distorted chain conformations induced by the proteins. Thus, our model appears to lead to a rather conventional interpretation of NMR spectra, for continuous variations with protein content and temperature without invoking the two-site point of view of Paddy et al.[18] A more complete discussion of these matters should be based upon detailed ^2H NMR line shape and relaxation studies using these models (cf. ref 22, 23, 48 and references they cite).

C. Summary. In summary, we believe our ESR simulations do show that a single phase (or one-site) model is a possible alternative to the more familiar two-site interpretation of ESR spectra involving protein–lipid interactions. It seems reasonable, at this stage, to suspect that the "one-site" model is more appropriate for some cases, while other cases are better characterized by a two (or greater) site model. Our primary point for now is that careful simulation of ESR spectra, based upon well-conceived microscopic models,[50] is called for in order to appreciate the range of possibilities consistent with the ESR spectra observed, and then carefully designed experiments are required to distinguish amongst them.[51]

Acknowledgment. We would like to thank Dr. G. Moro for his extensive help with and advice on the computer programs used in the simulations. This work was supported by NIH Grant GM25862 and by NSF Solid State Chemistry Grant DMR81-02047. E. M. acknowledges further support from the Charles H. Revson Foundation.

(50) These could include the idea of a coherence length for the range of the distorting effects of the protein on the lipid phase by analogy to liquid crystal theory.[27] Such a model would necessarily require inclusion of the translational diffusion of the lipids into and out of the range of the proteins.

(51) One such experiment, which leads to significantly increased spectral resolution, is to study well-aligned multibilayers (cf. H. Tanaka and J. H. Freed, to be published). Improved resolution of the spin relaxation can be achieved with the new two-dimensional electron-spin-echo technique (cf. G. Millhauser and J. H. Freed *J. Chem. Phys.*, in press; L. Kar, G. Millhauser, and J. H. Freed, *J. Phys. Chem.*, submitted for publication).

Energy Partitioning in the Reactions of Barium Atoms with Normal and Branched Alkyl Iodides and Dibromoalkanes

Kishore K. Chakravorty[†] and Richard B. Bernstein*[‡]

Department of Chemistry, Columbia University, New York, New York 10027 *(Received: March 1, 1984)*

Laser-induced fluorescence (LIF) measurements are reported of the vibrational-state distribution of the nascent BaX product molecules formed by the reaction of a Ba beam with a crossed molecular jet of an organic halide RX (X = I, Br). The target molecules were the monoiodoalkanes CH_3I, C_2H_5I, n-C_3H_7I, i-C_3H_7I, and t-C_4H_9I and the dibromoalkanes CH_2Br_2, CH_3CHBr_2, and $(CH_3)_2CBr_2$. For the normal iodide reactions, the BaI vibrational distributions are similar to those observed by Zare et al. for CH_3I, i.e., bell shaped with substantial population inversion. Those for the branched iodides are somewhat skewed. For the dibromoalkanes, the BaBr distributions are similar to those of Schultz et al. for CH_2Br_2, with skewing for the branched alkanes. The peak of the BaX vibrational distribution v_{max} (and the average vibrational energy of the BaX) increases with the exoergicity of the reaction (and the carbon number of the molecule), with v_{max} increasing from 39 to 51 across the iodide series and from 41 to 52 for the bromides. The average BaI vibrational energy ranges from 8.5 to 11.5 kcal mol^{-1}; for BaBr, from 13 to 15 kcal mol^{-1}. The products' relative translational energy distributions deduced from the LIF results all peak at energies of ca. 7 kcal mol^{-1}. Recoil momentum distributions are near Gaussian. For the iodide reactions, utilizing the difference between the energy of the highest populated BaI vibrational state and the total available energy, we can make an estimate of the sum of the average BaI rotational energy and the average internal energy of the product alkyl radical. This sum is found to be small (ca. 6.5 kcal mol^{-1}) and essentially constant for all the iodide reactions. On the basis of the LIF intensities, reaction cross sections for the iodides (relative to CH_3I) are estimated to be 1.6, 2.9, 1.9, and 1.5 for C_2H_5I, n-C_3H_7I, i-C_3H_7I, and t-C_4H_9I, respectively. These results, especially for the isomeric propyl iodides, are indicative of significant steric effects on reactivity.

I. Introduction

The reactions of methyl iodide with alkali- and alkaline-earth-metal atoms have been studied extensively by the molecular beam scattering method.[1] In addition to the early measurements of product (MI) angular distributions,[2] a wide range of molecular beam experiments have been carried out, including measurements of product recoil velocity and energy distributions,[3] collision energy dependence of differential[4] and integral reaction cross sections,[5] orientation dependence of reactivity,[6] rotational and polarization analysis (via electric deflection) of the MI product,[7] and MI vibrational-state distributions, via laser-induced fluorescence (LIF).[8]

These reactions are found to proceed via the classic "rebound" or impulsive mechanism.[9] Thus, the MI product molecules scatter mainly backward in the center of mass (CM) system and a substantial fraction of the reaction exoergicity goes into trans-

[†]Present address: National Semiconductor Corp., Santa Clara, CA 95051.
[‡]Present address: Department of Chemistry, University of California, Los Angeles, CA 90024.

(1) For a review, see M. R. Levy, *Prog. React. Kinet.*, **10**, 1 (1979).
(2) (a) D. R. Herschbach, *Faraday Discuss. Chem. Soc.*, No. **55**, 233 (1973); (b) R. B. Bernstein and A. M. Rulis, *ibid.*, **55**, 293 (1973); (c) S. M. Lin, C. A. Mims, and R. R. Herm. *J. Phys. Chem.*, **77**, 569 (1973).
(3) (a) A. M. Rulis and R. B. Bernstein, *J. Chem. Phys.*, **57**, 5497 (1972); (b) C. Ottinger, P. Strudler, S. J. Riley, R. M. Harris, and D. R. Herschbach, data presented in ref 2a; (c) C. M. Scholeen and R. R. Herm, *J. Chem. Phys.*, **65**, 5398 (1976).
(4) (a) M. E. Gersh and R. B. Bernstein, *J. Chem. Phys.*, **56**, 6131 (1972); (b) A. G. Urena and R. B. Bernstein, *ibid.*, **61**, 4101 (1974); (c) G. Rotzell, R. Viard, and K. Schügerl, *Chem. Phys. Lett.*, **35**, 353 (1975).
(5) (a) M. E. Gersh andd R. B. Bernstein, *J. Chem. Phys.*, **55**, 4661 (1971); (b) K. T. Wu, H. F. Pang, and R. B. Bernstein, *ibid.*, **68**, 1064 (1978).
(6) (a) P. R. Brooks and E. M. Jones, *J. Chem. Phys.*, **45**, 3499 (1966); (b) R. J. Beuhler, R. B. Bernstein, and K. H. Kramer, *J. Am. Chem. Soc.*, **88**, 5331 (1966); (c) R. J. Beuhler and R. B. Bernstein, *J. Chem. Phys.*, **51**, 5305 (1969); (d) D. H. Parker, K. K. Chakravorty, and R. B. Bernstein, *Chem. Phys. Lett.*, **86**, 113 (1982).

0022-3654/84/2088-3465$01.50/0